Available online at www.sciencedirect.com
ScienceDirect
Geochimica et Cosmochimica Acta 70 (2006) 5134–5145
Geochimica
www.elsevier.com/locate/gca

Kinetics of cadmium adsorption on aluminum precipitation products formed under the influence of tannate

G. Yu [a,b], U.K. Saha [a], L.M. Kozak [a], P.M. Huang [a,*]

[a] *Department of Soil Science, University of Saskatchewan, 51 Campus Drive, Saskatoon, Sask., Canada S7N 5A8S*
[b] *Institute of Soil Science, Chinese Academy of Sciences, Nanjing, China*

Received 8 December 2005; accepted in revised form 15 June 2006

Abstract

The impeding effects of organic substances on the crystallization of Al precipitation products have been studied for more than three decades. However, the impacts of organics-induced structural perturbation and the resultant surface alteration of Al transformation products on their kinetics and mechanisms of the adsorption of trace metals still remain to be uncovered. This paper describes the kinetics of Cd adsorption on the short-range-ordered (SRO) Al precipitation products formed under the influence of tannate. The kinetics of Cd adsorption on the SRO Al precipitation products formed in the presence of tannate at initial tannate/Al molar ratios (MRs) of 0, 0.001, 0.01 and 0.1 was studied at an initial Cd concentration of 0.89 μM, pH 5.5, background electrolyte of 10^{-2} M $NaNO_3$, and solid phase concentration of 0.08 g L^{-1} at 278, 288, 298 and 313 K using the conventional batch method. The results show that, among the six empirical kinetic models tested, the second-order rate equation best described the kinetic data. Cadmium adsorption on SRO Al precipitation products was a multi-step process involving an initial fast reaction (0.083–0.75 h) followed by a slow reaction (0.75–4 h). The structural perturbation of Al precipitation products by tannate and the resultant development of their microporosity and alteration of surface and charge properties substantially enhanced the rate constants of both the fast and slow reaction processes of Cd adsorption. The heat of activation values for the fast reaction ranged from 27 to 41 kJ mol^{-1}, indicating that diffusion is the rate-limiting step in Cd adsorption. Except for the Al precipitation products formed at a tannate/Al MR of 0 and 0.001, the heat of activation was >47 kJ mol^{-1} for the slow reaction, indicating that the rate-limiting step is a chemical process, which apparently involves bond breaking and formation on the surfaces of the SRO Al precipitation products. The pre-exponential factor, an index of the frequency of Cd collision with the surface of Al precipitation products, significantly increased with the increase of the initial tannate/Al MR, which is attributed to the development of microporosity and the increase in the specific surface area of the Al precipitation products formed under the influence of tannate ligands. The findings merit attention to the role of natural organics, which vary in the structure and functionality, in developing the microporous structure of Al precipitation products and the impact on the dynamics and mechanisms of Cd transformation and transport in natural environments.
© 2006 Elsevier Inc. All rights reserved.

1. Introduction

Cadmium (Cd) being more weakly bound to soil constituents compared to other trace metals is recognized as one of the most mobile trace metals circulating in the environment; it can readily enter the human food chain (McLaughlin and Singh, 1999; Kabata-Pendias, 2000; Adriano, 2001; Noonan et al., 2002; Satarug et al., 2003; Adams et al., 2004; Bergkvist et al., 2005; Krishnamurti et al., 2005). Its toxicity threatens human and animal health by causing kidney and liver dysfunction, weakening immune system, and adversely affecting reproduction (Chaney et al., 1999; Satarug et al., 2000). Cadmium can enter and accumulate in soils through agricultural application of sewage sludge and phosphate fertilizers, and via other anthropological activities like land disposal of metal-contaminated municipal and industrial wastes (McLaughlin and Singh, 1999; Krishnamurti et al., 2005). Concentrations of Cd in uncultivated and uncontaminated

---

[*] Corresponding author.
E-mail address: huangp@sask.usask.ca (P.M. Huang).

0016-7037/$ - see front matter © 2006 Elsevier Inc. All rights reserved.
doi:10.1016/j.gca.2006.06.1567

soils up to 100 cm depth average 0.2 mg kg^{-1} and are accumulated mostly in organic-rich Ap horizon (Nriagu, 1980). The bioavailability, toxicity, fate, and transport of heavy metals such as Cd in soils are largely controlled by adsorption–desorption reactions on the surface of soil colloidal materials (Bolton and Evans, 1996; Sparks, 2003; Basta et al., 2005; Huang and Gobran, 2005).

Aluminum, as the third most abundant element on the earth's surface, is ubiquitous in all mineral soils. Upon the release of Al from soil minerals to slightly acidic soil solutions and natural waters through chemical and biological weathering reactions, it undergoes hydrolysis processes (Huang et al., 2002), which results in the formation of Al hydroxides and oxyhydroxides occurring both as discrete particles and as coatings on the surface of other soil constituents (Sposito, 1996; Violante et al., 2002). In natural environments, pure Al precipitation products rarely exist. The hydrolysis of Al proceeds under the influence of many common soil-forming factors in the environment. Organic acids, released from plant roots or microbial activity, are an integral part of natural environments (Stevenson, 1994; Huang, 1995, 2004). The influence of organic acids on the structural distortion and surface alteration of Al precipitation products has been extensively investigated in the past three decades (Kwong and Huang, 1975, 1977, 1979a,b,c, 1981; Violante and Violante, 1980; Violante and Huang, 1984, 1985, 1989, 1993; Huang et al., 2002; Colombo et al., 2004).

A great deal of past research demonstrated that hydroxides/oxyhydroxides of Fe, Al, and Mn are important adsorbents of heavy metals in soils (Benjamin and Leckie, 1981; Kinniburgh and Jackson, 1981; Goh et al., 1986; Essington and Mattigod, 1991; Fu et al., 1991; Alloway, 1995; Bolton and Evans, 1996; Barrow, 1998; Gray et al., 1998; Lombi et al., 2002; Violante and Pigna, 2002; Sparks, 2003; Violante et al., 2003; Huang and Gobran, 2005; Zou et al., 2006). Hydroxides /oxyhydroxides of Al selectively adsorb divalent metal cations even at low pH values where these minerals are positively charged, suggesting the formation of chemical bonding (specific adsorption) rather than mere electrostatic association. Metal adsorption is often a fast stage reaction followed by a slow continuous reaction, which are apparently due to slow conversion from outer- to inner-sphere surface complexes (Jeon et al., 2003) and slow diffusion through micropore (Strawn et al., 1998). The combination of the pressure-jump relaxation, macroscopic kinetic study and X-ray absorption fine structure (XAFS) spectroscopy has demonstrated the formation of inner-sphere complexes during the two-step adsorption processes (Grossl et al., 1997; Strawn et al., 1998). In the specific adsorption of heavy metals by metal oxides, the formation of inner-sphere bonds results in direct contact between the metal ions and O atoms (Forbes et al., 1976; Goldberg et al., 1996; McBride, 1981, 2000; Manning et al., 1998; Arai et al., 2001; Ladeira et al., 2001; Reilly et al., 2001; Violante et al., 2002). The types of inner-sphere surface complexes formed on metal oxides such as goethite vary with the degree of surface coverage; at low-surface coverages, the monodentate complex is favored while at higher surface converages the bidentate complexes are more prevalent (Fendorf et al., 1997). Besides metal oxides, the role of phenolic OH and COOH groups of organic matter as metal-binding ligands has also been documented (Loneragan, 1975; Abd-Elfattah and Wada, 1981; Huang and Schnitzer, 1986; Stevenson, 1994; Huang, 2004). Some other studies demonstrated that the common rhizospheric organic acid ligands, when occurs simultaneously with heavy metals in solution, enhance metal adsorption by the various soils and clays (Naidu and Harter, 1998; Benyaha and Garnier, 1999; Taniguchi et al., 2000; Glover et al., 2002). Liu and Huang (2003) reported that Fe-oxides formed in the presence of citric acid at various citrate/Fe(II) molar ratios were poorly crystalline/noncrystalline, had greater specific surface, and lower ZPC and showed faster Pb adsorption kinetics relative to one formed in the absence of citrate. However, to date, little is known about the impact of the organics-induced structural perturbation and resultant surface alteration of Al precipitation products on the kinetics of adsorption of heavy metals. Therefore, the objective of this study was to investigate the kinetics of Cd adsorption on SRO Al precipitation products formed under the influence of tannic acid, which has both phenolic hydroxyl and carboxyl groups, at various concentrations common in natural environments. The effects of temperature on Cd adsorption kinetics were also included in this study to determine the pre-exponential factor (an index of the frequency of Cd collision with mineral surfaces) and the activation energy in the adsorption process.

2. Materials and methods

2.1. Synthesis of Al precipitation products

Aluminum precipitation products were formed by slowly titrating 7×10^{-3} M $AlCl_3$ solution having initial tannate/Al molar ratios (MRs) of 0, 0.001, 0.01 and 0.1 against 0.1 M NaOH solution up to an OH/Al molar ratio of 3.0 at the rate of 2.5 mL min^{-1}. Appropriate amount of tannic acid was used to adjust the initial tannate/Al molar ratios in the reaction systems. The suspensions of all the reaction systems were aged for 40 d at 25 °C. After aging, the suspensions were filtered by ultrafiltration with a Millipore filter membrane with the pore size of 0.1 μm in diameter and the precipitates were washed with deionized distilled water until the electrical conductivity of the filtrate was lower than 5 μS cm^{-1} and free of chloride tested by 0.1 M $AgNO_3$ solution. The precipitates were finally freeze dried.

2.2. Characterization of Al precipitation products

2.2.1. X-ray diffraction

The minerals formed in the Al precipitation products were identified by X-ray diffraction (XRD) on a Rigaku X-ray diffractometer (Model RU-200) with Fe–Kα radiation filtered by a graphite monochromator at 40 kV and

160 mA. The X-ray diffractograms were recorded from 4° to 60° with 0.02° 2θ steps at scanning rate of 10° 2θ per minute in continuous mode.

2.2.2. Aluminum contents

Aluminum precipitation products were digested with hydrofluoric acid in a closed vessel (Lim and Jackson, 1982) and the Al concentration in the digest was determined by atomic absorption spectrophotometry at a wavelength of 309.3 nm on Varian atomic absorption spectrophotometer (Model Spectr AA 220 Varian Australia Pty Ltd., Walnut Creek, CA).

2.2.3. Organic carbon contents

The organic carbon content of Al precipitation products was determined following dry combustion method of Wang and Anderson (1998) based on the loss of mass upon ignition at 850 °C using a Leco CR12 C analyzer (Leco Corp., St. Joseph, MI).

2.2.4. Specific surface area and surface porosity

The specific surface area of the Al precipitation products was measured by a gravimetric method based on the retention of ethylene glycol monoethyl ether (EGME) (Eltantawy and Arnold, 1973) and by using a multiple point Brunauer–Emmet–Teller (BET) N_2 adsorption isotherm (Gregg and Sing, 1982) obtained with one ASAP2000 Surface Area Analyzer (Micromeritics Instrument Corporation, Norcross, GA, USA). Prior to N_2 adsorption, around 200 mg of the samples were outgassed for 24 h at 10 mTorr. During N_2 adsorption the solids were thermostated in liquid N_2 (77–78 K). Also the pore specific surface area and average pore diameter of the Al precipitation products were determined from the N_2 adsorption isotherms using the t-plot method of de Boer and using the Kelvin equation (assuming cylindrical pores), respectively.

2.2.5. Point of zero salt effect

The point of zero salt effect (PZSE) of the Al precipitation products was determined by the modified salt titration method of Sakurai et al. (1988). The PZSE values were obtained by locating the point of intersection of pH difference (ΔpH) between before and after 2 M NaCl solution addition (to suspensions with various pHs) versus pH.

2.3. Cd adsorption kinetics experiments

The kinetics of Cd adsorption by Al precipitation products formed at initial tannate/Al molar ratios (MRs) of 0, 0.001, 0.01 and 0.1 was studied by the conventional batch method. The freeze-dried Al precipitation products were dispersed as suspension (81.64 mg L^{-1}) by ultrasonification (Sonifier, Model 350) at 150 W for 2 min. An aliquot of the suspension containing 8 mg of the Al precipitation products was transferred to a series of 250 mL flasks, and then shaken at 200 rpm for 24 h at 278, 288, 298 and 313 K on a shaker having a constant-temperature water bath. This pre-equilibration was conducted to prepare the reaction systems at respective temperatures. The pHs of the suspensions were then adjusted to 5.5 with 0.1 M HNO_3 or 0.1 M NaOH. An aliquot of 2 mL of a stock solution, containing 44.5 μM $Cd(NO_3)_2$ and 0.5 M $NaNO_3$ previously adjusted to pH 5.5, was added to each flask to obtain the initial Cd and $NaNO_3$ concentrations of 0.89 μM and 0.01 M, respectively. Thus, the final volume of the suspension was 100 mL. The concentration of Al precipitation products in the suspension was, thus, 0.08 g L^{-1}. The reaction vessels (flasks) were immediately transferred to the same shaker with a constant temperature water bath. The suspensions were shaken for 0.033, 0.083, 0.167, 0.333, 0.5, 0.75, 1, 2, 4, 8, 16 and 24 h. At the end of each reaction period, one of the reaction vessels was withdrawn from the shaker and its suspension was filtered through a 0.1-μm Millipore membrane within 15 s. The Cd concentration of the filtrates was determined by Graphite furnace-atomic absorption spectrometry (AAS) at a wavelength of 228.8 nm. The amount of Cd adsorbed was determined based on the difference between the initial and final concentrations of Cd in the solution. All the experiments were conducted in duplicate.

2.4. Statistical analyses of the Cd adsorption kinetics data

The linear forms of different kinetic equations were applied to the adsorption data and their goodness of fit was evaluated based on the r^2, level of significance (p), and standard error (SE). The comparisons of the amounts of Cd adsorbed, adsorption rate constants, activation energies, and pre-exponential factor values in different cases were carried out using the least significant difference (LSD) test. The LSD values were calculated based on SE and t values at appropriate degrees of freedom at 95% and 99% confidence levels. The LSD values for the rate constants and those of activation energies were calculated based on the standard errors of the slopes for the rate equation and Arrhenius equation, respectively. The LSD values for the pre-exponential factor were calculated based on the standard error of the intercept of the Arrhenius equation.

3. Results and discussion

3.1. Amounts of Cd adsorbed by Al precipitation products

The adsorption of Cd on the Al precipitation products formed at 4 different initial tannate/Al molar ratios (MRs) invariably reached a quasi-equilibrium at the end of a 24-h reaction period in the temperature range studied (Fig. 1).

The amounts of Cd adsorbed on the Al precipitation products formed at different MRs at the end of a 24-h reaction period at 4 different temperatures are given in Table 1. The amounts of Cd adsorbed on the different Al precipitation products formed at different MRs increased with the increase of temperature, because higher

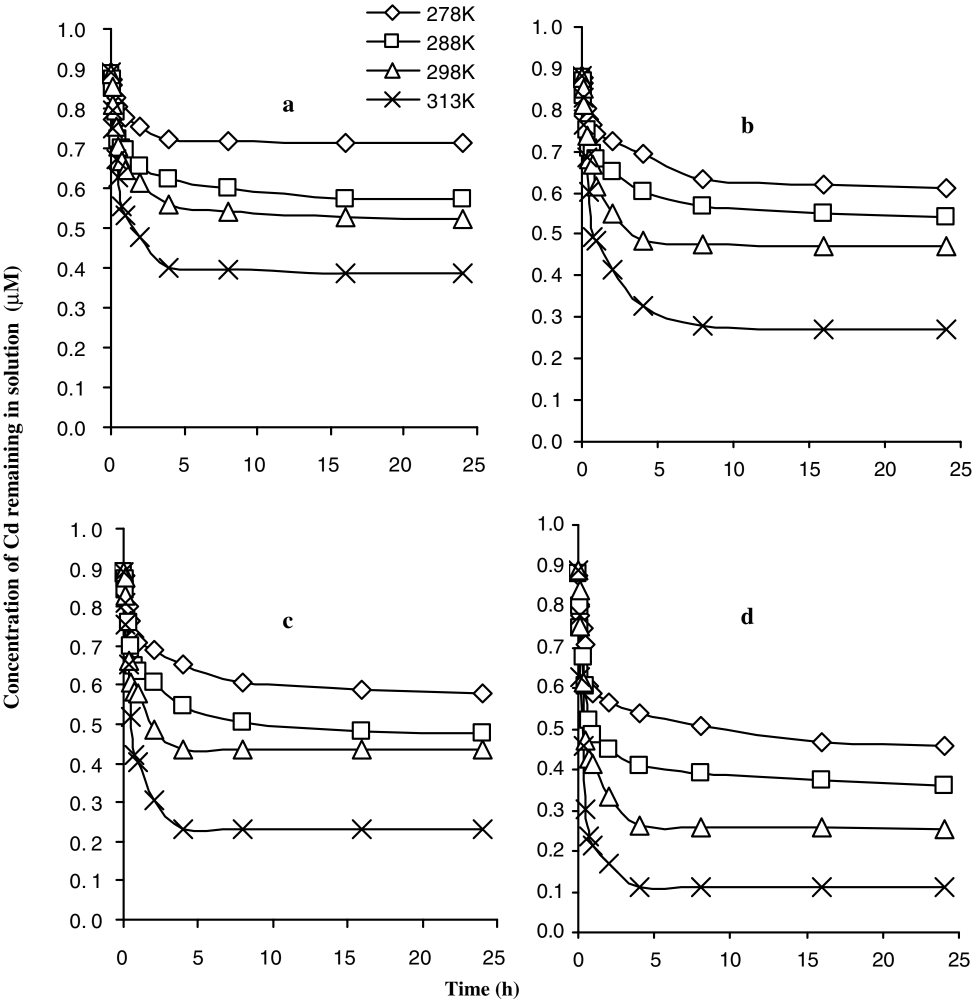

Fig. 1. Time function of Cd adsorption on the Al precipitation products formed at tannate/Al MRs of (a) 0, (b) 0.001, (c) 0.01 and (d) 0.1.

Table 1
The amounts of Cd adsorbed on Al precipitation products at the end of a 24-h reaction period at different temperatures

Initial tannate/ Al molar ratio	278 K	288 K	298 K	313 K	SE	$LSD_{0.05}$	$LSD_{0.01}$
	μmol Cd g^{-1}						
0	2.24 ± 0.06	4.05 ± 0.07	4.66 ± 0.08	6.41 ± 0.02	0.06	0.18	0.30
0.001	3.54 ± 0.05	4.42 ± 0.06	5.33 ± 0.04	7.92 ± 0.02	0.05	0.13	0.21
0.01	3.95 ± 0.20	5.24 ± 0.04	5.79 ± 0.03	8.42 ± 0.05	0.11	0.30	0.49
0.1	5.49 ± 0.17	6.74 ± 0.09	8.11 ± 0.06	9.93 ± 0.07	0.11	0.30	0.50
SE	0.14	0.07	0.06	0.05			
$LSD_{0.05}$	0.38	0.20	0.15	0.13			
$LSD_{0.01}$	0.64	0.34	0.25	0.21			

temperatures provided more energy to enhance the diffusion of Cd ions into the adsorbents and to break and form bonds on the surface of the Al precipitation products. Higher temperature could also enhance the rehydration of the Al precipitates to promote Cd adsorption. At all temperature conditions, the amounts of Cd adsorbed after 24 h reaction period on the Al precipitation products formed at various MRs followed the sequence of 0.1 > 0.01 > 0.001 > 0 (Table 1).

The differences in structural configuration, surface properties and porosity of the Al precipitation products formed at different initial tannate/Al MRs account for the significant differences of their Cd adsorption behavior. In the absence of tannic acid, the mixture of well crystalline Al precipitation products, including bayerite and gibbsite was formed (Fig. 2). The presence of tannic acid even at an initial tannate/Al MR of 0.001 perturbed the crystallization of the Al precipitation products and the

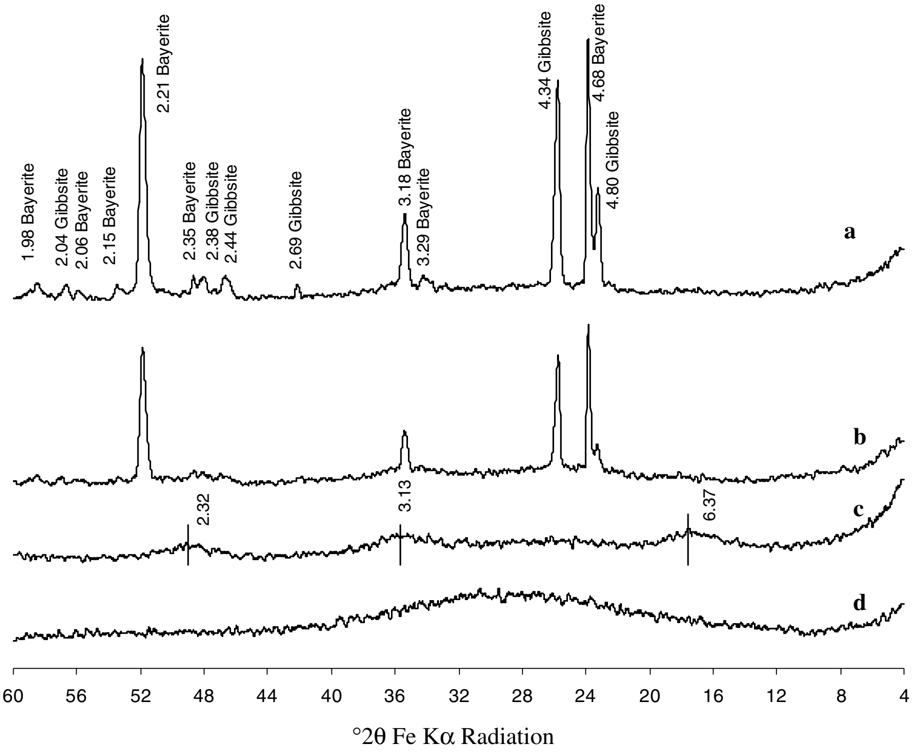

Fig. 2. X-ray diffractograms of Al precipitation products formed under the influence of tannate at tannate/Al molar ratios of (a) 0, (b) 0.001, (c) 0.01 and (d) 0.1 after 40 d aging. The *d*-values are in Å. The *d*-values of 2.32, 3.13 and 6.37 are characteristic peaks of boehmite.

resultant precipitates of Al were poorly crystalline. As the tannate/Al MR was increased to 0.01 and 0.1, the degree of crystallinity of the Al hydrolytic precipitates was further reduced and only X-ray noncrystalline products were formed (Fig. 2). The microporosity (<2 nm, Lowell and Shields, 1991) was developed and the average pore diameter decreased with increasing structural perturbation of the crystallization of the Al precipitation products by tannate, which was accompanied by the increase of their specific surface areas (Table 2). The Cd adsorption and the structural and surface properties of the Al precipitation products are closely related. The amount of Cd adsorbed in 24 h (Table 1) had positive correlations with the specific surface area ($r = 0.915$; $p = 0.085$) and micropore area ($r = 0.996$; $p = 0.004$), and negative correlations with average pore diameter ($r = -0.899$; $p = 0.101$) and PZSE ($r = -0.975$; $p = 0.025$) of the Al precipitation products formed at different MRs. Furthermore, the PZSE of the Al precipitation products decreased consistently with the increase of the tannate/Al MR (Table 2). Lower PZSE indicates more net negative surface charge exposed on the surface of the precipitation products at the same pH, and thus, has a greater capacity to adsorb Cd^{2+} ions. With the increase of the tannate/Al MR in the initial solution from 0.001 to 0.1, the organic C content of the Al precipitation products formed increased steadily and their tannate/Al MR values increased by two orders of magnitude (Table 2), which evidently contributed to the development of negative charge through exposure of organic functional groups such as carboxyl and phenolic hydroxyls on the Al precipitation products. Al precipitation products formed at higher tannate/Al MRs characterized with higher specific surface area, more porous surface and higher organic carbon contents, together with lower PZSE (Table 2), thus provide more active sites for Cd adsorption (Table 1).

Table 2
Characteristics of Al precipitation products formed at various initial tannate/Al MRs after 40 d aging

Characteristics of Al precipitation products formed	Tannate/Al molar ratio (MR) in the initial solution			
	0	0.001	0.01	0.1
BET specific surface area ($m^2\ g^{-1}$)	19.2 ± 0.3	109.2 ± 0.5	114.6 ± 0.5	185.9 ± 0.9
Micropore area ($m^2\ g^{-1}$)	0	12.0 ± 0.5	14.9 ± 0.1	43.8 ± 0.8
Average pore diameter (nm)	6.6 ± 0.3	5.0 ± 0.0	3.5 ± 0.1	2.4 ± .0.1
PZSE	9.9 ± 0.8	8.8 ± 0.3	7.2 ± 0.7	4.8 ± 0.4
Organic C ($g\ kg^{-1}$)	0	9.7 ± 0.7	113.1 ± 0.7	328.8 ± 1.4
Total Al ($g\ kg^{-1}$)	349 ± 10	333 ± 10	322 ± 17	155 ± 9
Tannate/Al MR[a]	0	0.0008	0.01	0.06

[a] Calculated based on the molecular weight (1701.20) of tannic acid ($C_{76}H_{52}O_{46}$).

3.2. Rate constants of Cd adsorption

The time functions of Cd adsorption on the Al precipitation products formed at different tannate/Al MRs at different temperatures are shown in Fig. 1. The time required to reach a quasi-equilibrium of Cd adsorption decreased with the increase of temperature. In the case of Al precipitation products formed at the tannate/Al MR of 0.1, the times required in reaching the quasi-equilibrium were 24, 16, 8 and 4 h at 278, 288, 298 and 313 K, respectively.

The steepness of the adsorption curves shows that Cd concentration in the solution generally decreased rapidly in the 0.083–0.75 h and slowly in the 0.75–4 h reaction periods (Fig. 1), indicating that Cd adsorption on the Al precipitation products was a multi-step process. Thus, the reaction kinetics of Cd adsorption in the present study was divided into an initial fast reaction (0.083–0.75 h) followed by a slow reaction (0.75–4 h). Such multi-step adsorption process was attributable to the heterogeneity of adsorption sites on the Al precipitation products. The site heterogeneity could be largely related to the different accessibility of surface pores with multiple sizes (Benjamin and Leckie, 1981; Heimestra et al., 1989). The surface carried locally positive (e.g., protonated OH; Al–OH_2^+) and negatively (e.g., deprotonated carboxyl group; Al–COO^-) charged sites which would act oppositely in electrostatically attracting Cd toward the surface. In any case, the adsorbed Cd would reduce the availability of the active binding sites including surface hydroxyl (Al–OH), phenolic hydroxyl, and carboxyl(–COOH), and lower the net surface negative charge. The electrostatic attraction for the adsorption of additional Cd ions was, thus, decreased due to the decreased surface negative charge on the reactive sites as adsorption proceeded (Shang et al., 1993; Liu and Huang, 2003; Saha et al., 2004).

Various kinetic and empirical equations, including the zero-order, first-order, second-order kinetic models, Elovich equation, parabolic diffusion equation and power function equation (Stumm and Morgan, 1996) were used to fit the Cd adsorption data. The degree of fit of the equations to the data was evaluated by correlation coefficient (r^2), level of significance (p), and standard error (SE) of model prediction obtained in the linear regression analyses. The values of these three parameters obtained by applying different models to the kinetic data obtained in the fast (0.083–0.75 h) and slow (0.75–4 h) reactions for four Al precipitates at 313 K are presented as an example in Table 3. The data indicate that all the models tested gave a linear relation with the p values <0.05. All equations fitted the data reasonably well except for power function equation which gave some extraordinarily higher SE values (>2 cmol kg^{-1}). This is in accord with the previous reports that in heterogeneous system, a number of rate equations often equally well describe the kinetics of a particular reaction, if correlation coefficients, level of significance and standard errors of the estimates are the indices to evaluate

Table 3
The comparison of the degree of fit of various kinetic models to the data of Cd adsorption by Al precipitation products, which were formed at different tannate/Al molar ratios (MRs), at 313 K

Model	MR = 0		MR = 0.001		MR = 0.01		MR = 0.1	
	Fr[a]	Sr[b]	Fr	Sr	Fr	Sr	Fr	Sr
				r^2				
Zero-order	0.915	0.982	0.984	0.989	0.976	0.942	0.917	0.974
First-order	0.950	0.991	0.997	0.996	0.992	0.971	0.978	0.996
Second-order	0.976	0.997	0.994	0.999	0.990	0.990	0.990	0.999
Elovich	0.985	0.993	0.928	0.981	0.926	0.993	0.975	0.958
Parabolic diffusion	0.981	0.998	0.995	0.997	0.990	0.979	0.985	0.908
Power function	0.749	0.999	0.933	0.989	0.800	0.990	0.810	0.954
				p				
Zero-order	2.8×10^{-3}	9.2×10^{-3}	9.4×10^{-5}	5.7×10^{-3}	2.2×10^{-4}	2.9×10^{-2}	2.7×10^{-3}	1.3×10^{-2}
First-order	9.3×10^{-4}	4.3×10^{-3}	4.6×10^{-6}	1.8×10^{-3}	2.3×10^{-5}	1.5×10^{-2}	1.8×10^{-4}	2.2×10^{-3}
Second-order	2.2×10^{-4}	1.3×10^{-3}	1.3×10^{-5}	5.7×10^{-4}	4.1×10^{-5}	5.0×10^{-3}	3.9×10^{-5}	5.6×10^{-4}
Elovich	8.2×10^{-5}	3.1×10^{-3}	2.0×10^{-3}	9.4×10^{-3}	2.1×10^{-3}	3.3×10^{-3}	2.4×10^{-4}	2.1×10^{-2}
Parabolic diffusion	1.4×10^{-4}	7.3×10^{-4}	9.5×10^{-6}	1.6×10^{-3}	3.4×10^{-5}	1.1×10^{-2}	8.7×10^{-5}	4.7×10^{-2}
Power function	2.6×10^{-2}	5.4×10^{-4}	1.7×10^{-3}	5.5×10^{-3}	1.6×10^{-2}	4.8×10^{-3}	1.4×10^{-2}	2.3×10^{-2}
				SE[c]				
Zero-order	0.510	0.146	0.260	0.130	0.395	0.330	1.070	0.136
First-order	0.437	0.106	0.149	0.078	0.230	0.238	0.488	0.066
Second-order	0.370	0.066	0.157	0.061	0.316	0.149	0.563	0.035
Elovich	0.212	0.085	0.555	0.167	0.697	0.112	0.590	0.185
Parabolic diffusion	0.243	0.041	0.146	0.068	0.249	0.201	0.459	0.275
Power function	2.470	0.037	0.837	0.115	3.480	0.136	5.200	0.204

[a] Fast reaction (0.083–0.75 h).

[b] Slow reaction (0.75–4 h).

[c] Standard error: $SE = [\sum (A - A*)]^2/(n - 2)]^{1/2}$, where A is the experimental value; A^* is the theoretical value based on modeling; n is the number of the data; the unit of SE is cmol kg^{-1}.

their degree of fit (Chien and Clayton, 1980; Martin and Sparks, 1983; Sparks and Jardine, 1984; Sparks, 1989; Aharoni et al., 1991; Sparks, 2003). The best fitting equation is not necessarily consistent with the nature of adsorption system; dissimilar processes could be fitted by the same model and similar processes are also fitted by different equations (Aharoni and Sparks, 1991). However, the parameters of the best fitting equation could provide some very important information on adsorption rates in different reaction systems.

The summarized values of correlation coefficients, level of significance and standard errors obtained by fitting different models to our kinetic data in the fast and slow reaction for the four Al precipitates at four temperatures were presented in Table 4. Among the six models tested, power function equation was firstly excluded because of the extremely high SE values. The parabolic diffusion equation had the highest mean r^2 and the second-order equation had the second highest mean r^2. The second-order equation had the lowest mean p value while Elovich equation had the second lowest mean p value. It is believed that normalized SE values should be a more important criterion to evaluate the model performance, as it is related to the closeness of the model predictions with the observed untransformed data (amount adsorbed per unit mass) (Saha et al., 2004). On the contrary, r^2 and p values for different models are generated through plotting the model-specific Y-values versus the X-values, either one or both of which are obtained through transformation of the original data. In this study, parabolic diffusion equation had the lowest mean SE value and the second-order equation had the second lowest mean SE value.

It has been reported that the parameters derived by the Elovich and power function equations are not well defined physicochemically and rate constants may not be obtained from these models (Kuo and Lotse, 1973; Bolan et al., 1985). The parabolic diffusion equation could only provide the "apparent" diffusion coefficients (Sparks, 1999). Among the ordered rate equations examined, the second-order equation gave the highest mean r^2 values and the lowest mean p and SE values (Table 4). Therefore, the second-order kinetic equation was chosen to describe the Cd adsorption on Al precipitation products formed at various initial tannate/Al MRs.

The second-order plots of Cd adsorption on the Al precipitation products formed at various tannate/Al MRs at 298 K were given as an example in Fig. 3. Based on the second-order plottings, the rate constants for the fast and slow reactions of Cd adsorption on the Al precipitation products formed at four different MRs at four different temperatures were calculated (Table 5). The rate constants of the fast reaction were 3- to 11-fold higher than those of slow reactions.

Increasing temperature resulted in a substantial increase in the rate constant of Cd adsorption by the Al precipitation products formed at four tannate/Al MRs (Table 5). This supports a speculation that the availability of more energy at higher temperatures would enhance the diffusion of Cd ions and breakage and formation of bonds on the hydroxide surface. Although our macroscopic data are not a definitive proof of such microscopic/molecular mechanisms, the macroscopic kinetic data are consistent with this explanation. At each particular temperature, the rate constants of both the fast and slow adsorption reactions of Cd substantially increased with the increase of the initial tannate/Al MRs: $0.1 > 0.01 > 0.001 > 0$ (Table 5).

The positive effects of the initial tannate/Al MR on the rate constants of Cd adsorption on the Al precipitation products (Table 5) can be interpreted based on the same reasonings as discussed in the section dealing with the amount of Cd adsorbed. The major alteration of structural, charge, and surface properties of Al precipitation products formed in the presence of tannate can be concisely summarized as: (i) increased tannate-induced perturbation of crystallization (Fig. 2) and the resultant increased frequency of edge surfaces and structural defect sites on the 001 faces, (ii) the decrease of the average pore diameter, the development of microporosity and the increase of the specific surface area (Table 2), and

Table 4
Summary of the range and mean values of r^2, p, and standard error (SE) for different kinetics models fitted to the data of the fast and slow reactions of Cd adsorption on Al precipitation products formed at different tannate/Al molar ratio (MRs) at four temperatures[a]

Model	r^2		p		SE (cmol kg^{-1})	
	Range	Mean	Range	Mean	Range	Mean
Zero-order	0.888–0.995	0.952	9.3×10^{-5}–4.7×10^{-2}	1.1×10^{-2}	0.04–1.07	0.30
First-order	0.904–0.997	0.965	4.6×10^{-6}–3.6×10^{-2}	8.1×10^{-3}	0.04–0.64	0.23
Second-order	0.919–0.999	0.973	1.2×10^{-5}–2.8×10^{-2}	6.0×10^{-3}	0.01–0.64	0.20
Elovich	0.879–0.993	0.952	8.2×10^{-5}–2.1×10^{-2}	6.4×10^{-3}	0.04–0.72	0.26
Parabolic diffusion	0.908–0.999	0.976	1.0×10^{-6}–4.7×10^{-2}	6.5×10^{-3}	0.02–0.49	0.17
Power function	0.749–0.999	0.944	8.0×10^{-5}–2.6×10^{-2}	7.9×10^{-3}	0.04–5.20	0.73

[a] For any kinetic model, the values presented here were obtained through applying the model separately to the individual kinetic data for both the fast and slow reactions in four Al precipitation products at each temperature, i.e., 278, 288, 298, and 313 K. The data obtained at 313 K are presented in Table 3. Those obtained at other three temperatures along with the data in Table 3 are summarized in this table to show the range and mean values of r^2, p and SE.

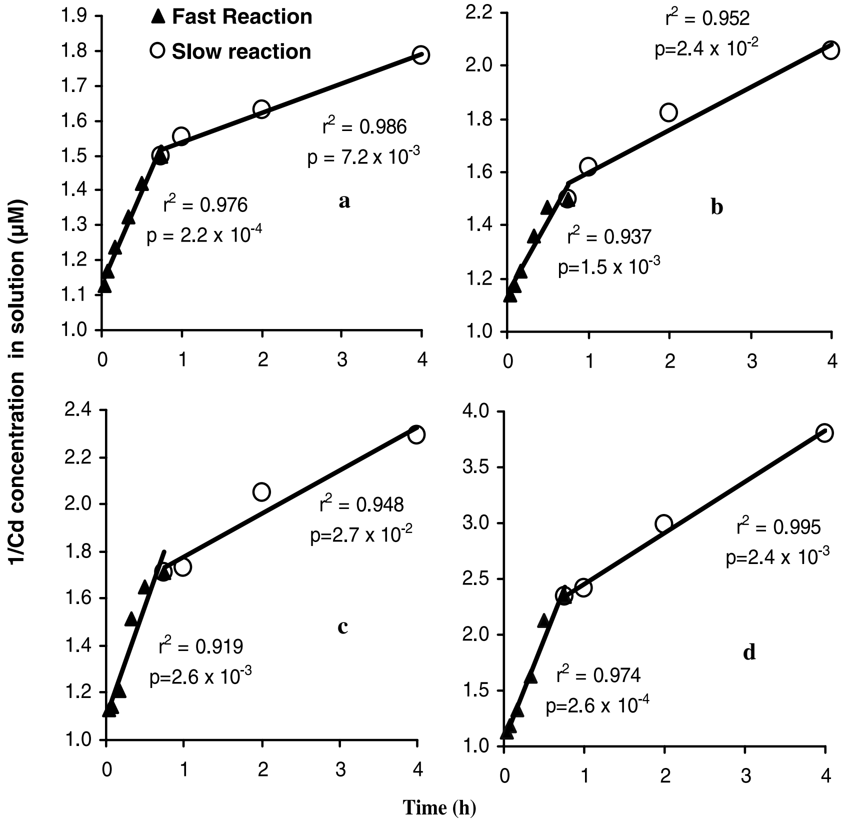

Fig. 3. The second-order plotting of Cd adsorption on the Al precipitation products formed at tannte/Al MRs of (a) 0, (b) 0.001, (c) 0.01 and (d) 0.1 at 298 K.

Table 5
The reaction rate constants of Cd adsorption on Al precipitation products formed at various tannate/Al molar ratios (MRs) at different temperatures, based on the second-order rate equation

	MR	278 K	288 K	298 K	313 K	SE	$LSD_{0.05}$	$LSD_{0.01}$
		[Rate constants $(M^{-1}\ h^{-1})] \times 10^{-4a}$						
Fast reaction	0	22.02	44.76	51.87	88.35	4.29	11.90	19.77
	0.001	27.84	47.11	54.40	119.93	4.90	13.59	22.54
	0.01	37.63	61.25	91.94	173.05	7.27	20.18	33.46
	0.1	63.34	105.48	182.32	451.72	10.65	29.56	49.03
SE		5.60	6.13	5.53	10.45			
$LSD_{0.05}$[b]		15.54	17.01	15.36	29.00			
$LSD_{0.01}$		25.78	28.21	25.47	48.10			
Slow reaction	0	3.05	5.86	8.38	21.18	0.99	2.75	4.57
	0.001	3.56	6.55	16.05	32.8	1.05	2.92	4.85
	0.01	4.36	8.51	18.29	59.67	1.19	3.31	5.48
	0.1	5.65	14.48	45.49	141.73	1.21	3.36	5.57
SE		0.48	0.54	0.86	1.93			
$LSD_{0.05}$		1.32	1.50	2.40	5.35			
$LSD_{0.01}$		2.19	2.49	3.98	8.87			

[a] The rate constants, SE and LSD values denoted in this table should be multiplied by 10^4.

[b] LSD calculation: The LSD values were calculated based on the SE and t values at appropriate degrees of freedom at 95% and 99% confidence levels; the LSD values for the rate constants were calculated based on the SE values of the slopes for the second-order rate equation.

(iii) higher organic C contents in the Al precipitation products formed in the higher initial tannate/Al MRs (Table 2), which provided more organic functional group such as carboxyl–COOH and phenolic hydroxyl–OH, and (iv) the drastic decrease of the PZSE (Table 2) and the resultant enhancement of the negative charge of the Al precipitates formed. Such alteration of structural, charge, and surface properties of the Al precipitation products due to tannate incorporation in their structure promoted their Cd adsorption kinetics.

3.3. Activation energy and pre-exponential factor of Cd adsorption

The effects of temperature on the rate constants of Cd adsorption on the Al precipitation products was investigated in more detail by determining the activation energy and pre-exponential factor using the Arrhenius equation Eq. (1) (Moore and Pearson, 1981):

$$k = A\mathrm{e}^{-Ea/RT} \tag{1}$$

where k is the rate constant, A is the pre-exponential factor (frequency factor), Ea is the Arrhenius activation energy, R is the universal gas constant ($8.314\ \mathrm{J\ K^{-1}}$), and T is the absolute temperature. Logarithmic transformation of Eq. (1) yields the following equation:

$$\ln k = A - Ea/RT \tag{2}$$

Plotting ln k (y-axis) versus $1/T$ (x-axis) yields a straight line, from which Ea and A can be obtained based on the slope and intercept, respectively.

Arrhenius plots of Cd adsorption kinetics on the Al precipitation products formed at different tannate/Al MRs were illustrated in Fig. 4. The data show that the Arrhenius equation fitted all the Cd adsorption processes very well ($p < 0.05$) with r^2 values ranging from 0.948 to 0.999.

The activation energy for Cd adsorption on the Al precipitation products ranged from 27 to 68 kJ mol^{-1} (Table 6). At various tannate/Al MRs, the activation energy for the slow reaction was 44–74% higher than that for the respective fast reaction, which is statistically significant at the 1% level. As the adsorption proceeded, more exposed and active reactive sites were occupied by Cd. Further adsorption of Cd would require diffusion of Cd ions to the less exposed sites such as micropores and also require more energy to break and form bonds on the Al precipitation products.

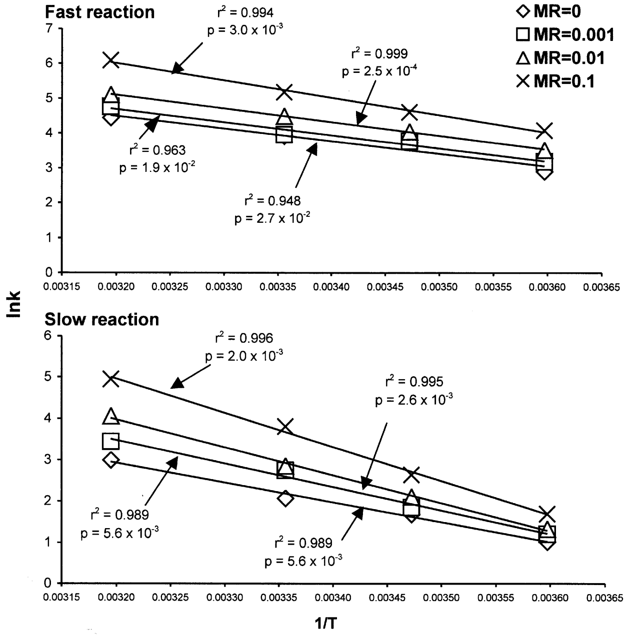

Fig. 4. Arrhenius plots of Cd adsorption kinetics on the Al precipitation products formed at different tannate/Al molar ratios (MRs), where k is the second-order rate constant ($\mathrm{M^{-1}\ h^{-1}}$) and T is absolute temperature (K).

For the fast reactions, the heat of activation values of Cd adsorption shows the trend of the increase with the increase of the initial tannate/Al MR. For the slow reaction, the heat of activation significantly increased with the increase of the initial tannate/Al MR: $0.1 > 0.01 > 0.001 > 0$. It is well-known that in heterogeneous systems such as mineral-water interfaces, diffusion occurs not only in the bulk solution but also in micropores, mesopore and macropores, in the films around solid particles (Sparks, 1989). Film diffusion typically has an activation energy value of 17 to 21 kJ mol^{-1} and intraparticle diffusion has an activation energy of 21 to 42 kJ mol^{-1} (Sparks, 1999). Low activation energy values (<42 kJ mol^{-1}) indicates diffusion-controlled processes whereas higher activation energy values (>42 kJ mol^{-1}) indicate chemically controlled processes (Sparks, 1989). The heat of activation values (Table 6) in the present study indicate that the rate-limiting step in adsorption reactions of Cd was basically a diffusion process for the Al precipitation products formed in the absence of tannic acid. The fast reaction of Cd adsorption by the Al precipitation products formed at tannate/Al MR of 0.001 was the diffusion-controlled process, whereas the slow reaction was the transitional case between the diffusion-controlled and chemical-controlled processes, since the heat of activation of 47 k mol^{-1} was the borderline case between these two processes. By contrast, a fast diffusion-controlled process followed by a chemically controlled process was true for the Al precipitation products formed in the presence of tannic acid at tannate/Al MRs of 0.01 and 0.1. It is believed that more activation energy is required for the diffusion of Cd ions to micropores than to large pores. The increase in the heat of activation for the slow reaction of the Cd adsorption with the increase of the initial tannate/Al MR (Table 6) is in accord with the decrease of average pore size and the development of microporosity of the Al precipitation products (Table 2).

The pre-exponential factor, an index of the frequency of collision of Cd with reactive sites on the Al precipitation products, increased by 3 and 5 orders of magnitude in the fast and slow reactions, respectively, with the increase of the initial tannate/Al MR from 0 to 0.1 (Table 6). The effects of the initial tannate/Al MR on the pre-exponential factor was significant at 1% level. With the increase of the tannate/Al MR, the Al precipitation products formed became less crystalline and eventually noncrystalline when the MR was increased to 0.01 and 0.1; the decrease in the crystallinity of the Al precipitation products resulted in the substantial increase in their specific surface area (Table 2). The poorly crystalline or noncrystalline Al precipitation products showed fluffy extensive and damaged surface (Kwong and Huang, 1979c). Thus, relative to a well crystalline Al precipitation product, more edges and corners as well as defect sites on the 001 faces exist in the rougher surfaces of poorly crystalline and non crystalline products.

Table 6
The activation energy and pre-exponential factor values of Cd adsorption on Al precipitation products formed at various initial tannate/Al molar ratios (MRs), based on the second-order rate constants

Tannate/Al MR	Activation Energy (kJ mol^{-1})[a]		Pre-exponential factor (M^{-1} h^{-1})[b]	
	Fast reaction	Slow reaction	Fast reaction	Slow reaction
0	27	39	5.4×10^{12}	6.9×10^{13}
0.001	29	47	7.1×10^{12}	2.6×10^{15}
0.01	31	54	2.9×10^{13}	8.6×10^{16}
0.1	41	68	2.6×10^{15}	2.9×10^{18}

[a] $LSD_{0.05} = 5.1$ and $LSD_{0.01} = 7.4$ for the activation energy (*E*a).
[b] $LSD_{0.05} = 6.0 \times 10^{10}$ and $LSD_{0.01} = 8.7 \times 10^{10}$ for the pre-exponential factor.

Compared with the well crystalline Al precipitation products formed in the absence of tannic acid, the poorly crystalline Al precipitation products formed at the tannate/Al MR of 0.001 and noncrystalline Al precipitation products formed at the tannate/Al MRs of 0.01 and 0.1 would bear more exposed Al–OH and Al–OH_2 groups at the edges and corners as well as at the defective sites on the 001 faces per unit area as Cd adsorption sites. Since tannate is incorporated in the short-range ordered Al precipitation products, some exposed Al atoms may also be bound with tannate which contains exposed phenolic hydroxyl and carboxyl functional groups; these are also potential Cd adsorption sites. In any case, perturbation of crystallization of Al precipitation products by tannate would enhance the collision frequency of Cd ions with their reactive sites, bringing about the higher pre-exponential factor. A differentiation between the bonding of Cd with Al–OH surface functional groups and that of Cd with Al-tannate functional groups based on the kinetics parameters is not possible and, thus, merits future research.

4. Conclusions

Structural perturbation of Al precipitation products by organic substances has been well documented (Kwong and Huang, 1975; Lind and Hem, 1975; Kodama and Schnitzer, 1980; Violante and Huang, 1984, 1985; Sposito, 1996; Huang et al., 2002; Colombo et al., 2004). However, the effects of the resulting alteration of structural and surface properties of Al precipitation products by organics on the kinetics and mechanisms of their adsorption of trace metals still remain unknown.

The present study presents the first report on original investigation describing the alteration of Cd adsorption kinetics on the Al precipitation products formed under the influence of organics such as tannate ligands which are present in soils and waters. The results reveal that the Cd adsorption kinetics and capacity on the Al precipitation products substantially increase with the increase of the initial tannate/Al molar ratio. This is attributed to structural perturbation of the Al precipitation products by tannate and the resultant development of microporosity, the decrease of the average pore diameter, the increase of specific surface area, exposed organic functional groups of the tannate incorporated to the surface and structural network of the precipitation products, and the decrease of their PZSE. The activation energy values indicate that the rate-limiting steps of the Cd adsorption is basically a diffusion-controlled process for the Al precipitation products formed in the absence of tannate, whereas a diffusion-controlled process followed by a chemically controlled process is evident for the Al precipitation products formed under the sufficient influence of tannate ligands (tannate/Al MR $\geqslant$ 0.01). The pre-exponential factor values, which indicate the collision frequency of Cd ions with the reactive sites, dramatically increase with increasing the degree of structural perturbation of Al precipitation products by tannate and the consequent development of their microporosity and the increase of their specific surface area.

The data obtained in the present study indicate that the role of organics, which vary in the structure and functionality and are common in natural environments, in exerting the structural perturbation of Al transformation products and the resultant alteration of their microporous structures, and surface and charge properties and the impact on dynamics and mechanisms of Cd transformation and transport in soils and waters deserves increasing attention.

Acknowledgment

This research was supported by Discovery Grant 2383-Huang of the Natural Sciences and Engineering Research Council of Canada.

Associate editor: Donald L. Sparks

References

Abd-Elfattah, A., Wada, K., 1981. Adsorption of lead, copper, zinc, cobalt, and cadmium by soils that differ in cation exchange materials. *J. Soil Sci.* **32**, 271–283.

Adams, M.L., Zhao, F.J., McGrath, S.P., Nicholson, F.A., Chambers, B.J., 2004. Predicting cadmium concentrations in wheat and barley grain using soil properties. *J. Environ. Qual.* **33**, 532–541.

Adriano, D.C., 2001. *Trace elements in terrestrial environments: biogeochemistry, bioavailability, and risks of heavy metals*. Springer-Verlag, New York, p. 846.

Aharoni, C., Sparks, D.L., 1991. Kinetics of soil chemical reactions—A theoretical treatments. In: Sparks, D.L., Suarez, D.L. (Eds.), *Rate of Soil Chemical Processes*. SSSA, Madison, WI, pp. 1–18, SSSA Spec. Pub. No. 27.

Aharoni, C., Sparks, D.L., Levinson, S., Ravina, I., 1991. Kinetics of soil chemical reactions: relationship between empirical equations and diffusion models. *Soil Sci. Soc. Am. J.* **55**, 1307–1312.

Alloway, B.J., 1995. Cadmium. In: Alloway, B.J. (Ed.), *Heavy Metals in Soils*. Blackie Academic and Professional, London, pp. 122–151.

Arai, Y., Elzinga, E.J., Sparks, D.L., 2001. X-ray absorption spectroscopic investigation of arsenite and arsenate adsorption at the aluminum oxide–water interface. *J. Colloid Interface Sci.* **235**, 80–88.

Barrow, N.J., 1998. Effects of time and temperature on the sorption of cadmium, zinc, cobalt, and nickel by a soil. *Aust. J. Soil Res.* **36**, 941–950.

Basta, N.T., Ryan, J.A., Chaney, R.L., 2005. Trace element chemistry in residual-treated soil: key concepts and metal bioavailability. *J. Environ. Qual.* **34**, 49–63.

Benjamin, M.M., Leckie, J.O., 1981. Multiple-site adsorption of Cd, Cu, Zn and Pb on amorphous iron oxyhydroxides. *J. Colloid Interf. Sci.* **79**, 209–221.

Benyaha, L., Garnier, J., 1999. Effect of salicyclic acid upon trace metal sorption (Cd, Zn, Co, and Mn) onto alumina, silica, and kaolinite as a function of pH. *Environ. Sci. Technol.* **33**, 1398–1407.

Bergkvist, P., Berggren, D., Jarvis, N., 2005. Cadmium solubility and sorption in a long-term sludge amended arable soil. *J. Environ. Qual.* **34**, 1530–1538.

Bolan, N.S., Barrow, N.J., Posner, A.M., 1985. Describing the effect of time on sorption of phosphate by iron and aluminum hydroxides. *J. Soil Sci.* **36**, 187–197.

Bolton, K.A., Evans, L.J., 1996. Cadmium adsorption capacity of selected Ontario soils. *Can. J. Soil Sci.* **76**, 183–189.

Chaney, R.L., Ryan, J.A., Li, Y.-M., Brown, S.L., 1999. Soil cadmium as a threat to human health. In: McLaughlin, M.J., Singh, B.R. (Eds.), *Developments in Plant and Soil Sciences*. Kluwer Academic Publishers, Dordrecht, The Netherlands, pp. 219–256.

Chien, S.H., Clayton, W.R., 1980. Application of Elovich equation to the kinetics of phosphate release and sorption in soils. *Soil Sci. Soc. Am. J.* **44**, 265–268.

Colombo, C., Ricciardella, M., Cerce, A.D., Maiuro, L., Violante, A., 2004. Effects of tannate, pH, sample preparation, ageing and temperature on the formation and nature of Al oxyhydroxides. *Clays Clay Miner.* **52**, 721–733.

Eltantawy, I.M., Arnold, P.W., 1973. Reappraisal of ethylene glycol mono-ethyl ether (EGME) method for surface area estimations of clays. *J. Soil Sci.* **24**, 232–238.

Essington, M.E., Mattigod, S.V., 1991. Trace element solid-phase associations in sewage sludge and sludge-amended soil. *Soil Sci. Soc. Am. J.* **55**, 350–356.

Fendorf, S., Eick, M.J., Grossl, P., Sparks, D.L., 1997. Arsenate and chromate retention mechanisms on goethite. 1. Surface structure. *Environ. Sci. Technol.* **31**, 315–320.

Forbes, E.A., Posner, A.M., Quirk, J.P., 1976. The specific adsorption of divalent Cd, Co, Cu, Pb, and Zn on goethite. *J. Soil Sci.* **27**, 154–166.

Fu, G., Allen, H.E., Cowan, C.E., 1991. Adsorption of cadmium and copper by manganese oxide. *Soil Sci.* **152**, 72–81.

Glover II, L.J., Eick, M.J., Brady, P.V., 2002. Desorption kinetics of cadmium^{2+} and lead^{2+} from goethite: influence of time and organic acids. *Soil Sci. Soc. Am. J.* **66**, 797–804.

Goh, B.T., Violante, A., Huang, P.M., 1986. Influence of tannic acid on retention of copper and zinc by aluminum precipitation products. *Soil Sci. Soc. Am. J.* **50**, 820–825.

Goldberg, S., Davis, J.A., Hem, J.D., 1996. The surface chemistry of aluminum oxides and hydroxides. In: Sposito, G. (Ed.), *The Environmental Chemistry of Aluminum*. CRC Press, Boca Raton, FL, pp. 271–330.

Gray, C.W., McLaren, R.G., Roberts, A.H.C., Condron, L.M., 1998. Sorption and desorption of cadmium from some New Zealand soils: effects of pH and contact time. *Aust. J. Soil Res.* **36**, 199–216.

Gregg, S.L., Sing, K.S.W., 1982. *Adsorption Surface Area and Porosity*, second ed. Academic Press, London.

Grossl, P.R., Eick, M., Sparks, D.L., Goldberg, S., Ainsworth, C.C., 1997. Arsenate and chromate retention mechamisms on goethite. 2. Kinetics evaluation using a pressure-jump relaxation technique. *Environ. Sci. Technol.* **31**, 321–326.

Heimestra, T., van Riemsdijek, W., Bolt, H., 1989. Multisite proton adsorption modeling at the solid/solution interface of (hydr)oxides. *J. Colloid Interface Sci.* **133**, 104–107.

Huang, P.M., 1995. The role of short range ordered mineral colloids in abiotic transformation of organic components in the environment. In: Huang, P.M. et al. (Eds.), *Environmental Impact of Soil Component Interactions*. Lewis Publishers, Bocan Raton, FL, pp. 135–167.

Huang, P.M., 2004. Soil mineral–organic matter–microorganism interactions: fundamentals and impacts. *Adv. Agron.* **82**, 391–472.

Huang, P.M., Gobran, G., 2005. *Biogeochemistry of trace elements in the rhizosphere*. Elsevier, Amsterdam, The Netherlands, 465p.

Huang, P.M., Schnitzer, M., 1986. Interactions of soil minerals with natural organics and microbes. SSSA Spec. Publ. 17. Soil Sci. Soc. Am., Madison, WI.

Huang P.M., Wang, M.K., Kampe, N., Schulze, D.G., 2002. Aluminum hydroxides. In: Dixon, J.B., Schutze, D.G. (Eds.), Soil Mineralogy with Environmental Applications, SSSA Book Series, No.7. Soil Sci. Soc. Am., Madison, WI, pp. 261–289.

Jeon, B-H., Dempsey, B.A., Burgos, W.D., Royer, R.A., 2003. Sorption kinetics of Fe(II), Zn(II), Co(II), Ni(II), Cd(II) and Fe(II)/Me(II) onto hematite. *Water Res.* **37**, 4135–4142.

Kabata-Pendias, A., 2000. *Trace Elements in Soils and Plants*. CRC Press, Bocan Raton, FL, 413p.

Kinniburgh, D.G., Jackson, M.L., 1981. Cation adsorption by hydrous metal oxides and clays. In: Anderson, M.A., Rubin, A.S. (Eds.), *Adsorption of Inorganics at Solid–liquid Interphases*. Ann Arbor Science, Ann Arbor, MI, pp. 91–160.

Kodama, H., Schnitzer, M., 1980. Effect of fulvic acid on the crystallization of aluminum hydroxides. *Geoderma* **24**, 195–205.

Krishnamurti, G.S.R., McArthur, D.F.E., Wang, M.K., Kozak, L.M., Huang, P.M., 2005. Biogeochemistry of soil cadmium and the impact on terrestrial food chain contamination. In: Huang, P.M., Gobran, G. (Eds.), *Biogeochemistry of Trace Elements in the Rhizosphere*. Elsevier, Amsterdam, The Netherlands, pp. 197–257.

Kuo, S., Lotse, E.G., 1973. Kinetics of phosphate adsorption and desorption by hematite and gibbsite. *Soil Sci.* **116**, 400–406.

Kwong Ng Kee, K.F., Huang, P.M., 1975. Influence of citric acid on the crystallization of Al precipitation products. *Clays Clay Miner.* **23**, 164–165.

Kwong Ng Kee, K.F., Huang, P.M., 1977. Influence of citric acid on the hydrolytic reactions of aluminum. *Soil Sci. Soc. Amer. J.* **41**, 692–697.

Kwong Ng Kee, K.F., Huang, P.M., 1979a. Surface reactivity of aluminum hydroxides precipitated in the presence of low molecular weight organic acids. *Soil Sci. Soc. Am. J.* **43**, 1107–1113.

Kwong Ng Kee, K.F., Huang, P.M., 1979b. The relative influence of low-molecular-weight, complexing organic acids on the hydrolysis and precipitation of aluminum. *Soil Sci.* **128**, 337–342.

Kwong Ng Kee, K.F., Huang, P.M., 1979c. Nature of hydrolytic precipitation products of aluminum as influenced by low-molecular-weight complexing organic acids. In: Mortland, M.M., Farmer, V.C. (Eds.), *Proceedings of the VI International Clay Conference 1978*. Elsevier Scientific Publishing company, Amsterdam, the Netherlands, pp. 527–536.

Kwong Ng Kee, K.F., Huang, P.M., 1981. Comparison of the influence of tannic acid and selected low-molecular-weight organic acids on precipitation products of aluminum. *Geoderma* **26**, 179–183.

Ladeira, A.C.Q., Ciminelli, V.S.T., Duarte, H.A., Alves, M.C.M., Ramos, A.Y., 2001. Mechanism of anion retention from EXAFS and density functional calculations: arsenic (V) adsorbed on goethite. *Geochim. Cosmochim. Acta* **65**, 1211–1217.

Lim, C.H., Jackson, M.L., 1982. Dissolution of total elemental analysis. In: Page, A.L. (Ed.), Methods of Soil Analysis, Part 2 Chemical and Microbiological Properties, second ed., Am. Soc. Agron. and Soil Sci. Soc. Am., Madison, WI, USA, pp. 1–12.

Lind, C.J., Hem, J.D., 1975. Effects of organic solutes on chemical reactions of aluminum. *U. S. Geol. Surv. Water Supply Paper*, 1827-G.

Liu, C., Huang, P.M., 2003. Kinetics of lead adsorption by iron oxides formed under the influence of citrate. *Geochim. Cosmochim. Acta* **67**, 1045–1054.

Lombi, E., Zhao, G., Zhang, B., Fitz, W., Zhang, H., McGarth, S.P., 2002. In situ fixation of metals in soils using bauxite residue: chemical assessment. *Environ. Pollut.* **118**, 435–443.

Loneragan, J.F., 1975. The availability and adsorption of trace elements in soil–plant systems and their relation to movement and concentrations of trace elements in plants. In: Nicholas, D.J.D., Egan, A.R. (Eds.), Trace Elements in Soil–plant–animal Systems, Proc. Jubilee Symp. Waite Agric. Res. Inst., Glen Osmond, South Australia, 5–6 November 1974, Academic Press, New York, pp. 109–134.

Lowell, S., Shields, J.E., 1991. *Powder surface area and porosity*, third ed. Chapman and Hall, New York.

Manning, B.A., Fendorf, S.E., Goldberg, S., 1998. Surface structures and stability of arsenic (III) on goethite: spectroscopic evidence for inner-sphere complexes. *Environ. Sci. Technol.* **32**, 2383–2388.

Martin, H.W., Sparks, D.L., 1983. Kinetics of nonexchangeable potassium release from two Coastal Plain soils. *Soil Sci. Soc. Am. J.* **47**, 883–887.

McBride, M.B., 1981. Forms and distribution of copper in solid and solution phases of soil. In: Loneragan, J.F. et al. (Eds.), *Copper in Soils and Plants*. Academic Press, New York, pp. 25–45.

McBride, M.B., 2000. Chemisorption and precipitation reactions. In: Sumner, M.E. (Ed.), *Handbook of Soil Science*. CRC Press, Boca Raton, FL, pp. B265–B302.

McLaughlin, M.J., Singh, B.R., 1999. Cadmium in soils and plants. In: McLaughlin, M.J., Singh, B.R. (Eds.), *Cadmium in Soils and Plants, Developments in Plant and Soil Sciences*. Kluwer Academic Publishers, Dordrecht, The Netherlands, pp. 1–7.

Moore, J.W., Pearson, R.G., 1981. *Kinetics and Mechanism*, 3rd ed. John Wiley and Sons, New York.

Naidu, R., Harter, R.D., 1998. Effect of different organic ligands on cadmium sorption by and extractability from soils. *Soil Sci. Soc. Am. J.* **62**, 644–650.

Noonan, C.W., Sarasua, S.M., Campagna, D., Kathman, S.J., Lybarger, J.A., Mueller, P.W., 2002. Effects of exposure to low levels of environmental Cd on renal biomarkers. *Environ. Health Perspectives* **110**, 151–155.

Nriagu, J.O., 1980. Part 1: Ecological cycling. In: Nriagu, J.O. (Ed.), *Cadmium in the Environment*. Wiley Interscience, New York, pp. 2–12.

Reilly, S.E., Strawn, D.G., Sparks, D.L., 2001. Residence time effects on arsenate adsorption/desorption mechanisms on goethite. *Soil Sci. Soc. Am. J.* **65**, 67–77.

Saha, U.K., Liu, C., Kozak, L.M., Huang, P.M., 2004. Kinetics of selenite adsorption on hydroxyaluminum- and hydroxyaluminosilicate–montmorillonite complexes. *Soil Sci. Soc. Am. J.* **68**, 1197–1209.

Sakurai, K., Ohadate, Y., Kyuma, K., 1988. Comparison of salt titration and potentiometric titration methods for the determination of zero point of charge (ZPC). *Soil Sci. Plant Nutr.* **34**, 171–182.

Satarug, S., Baker, J.R., Urbenjapol, S., Haswell-Elkins, M., Reilly, P.E.B., Williams, D.J., Moore, M.R., 2003. A global perspective on Cd pollution and toxicity in non-occupationally exposed population. *Toxicol. Lett.* **137**, 65–83.

Satarug, S., Haswell-Elkins, M.R., Moore, M.R., 2000. Safe levels of cadmium intake to prevent renal toxicity in human subject. *British J. Nutr.* **84**, 791–802.

Shang, C., Huang, P.M., Stewart, J.W.B., 1993. Kinetics of adsorption of organic and inorganic phosphates by short-range ordered iron precipitate. *Soil Sci. (Trends Agri. Sci.)* **1**, 137–144.

Sparks, D.L., 1989. *Kinetics of Soil Chemical Processes*. Academic Press, New York.

Sparks, D.L., 1999. Kinetics of sorption/release reactions at the soil mineral/water interface. In: Sparks, D.L. (Ed.), *Soil Physical Chemistry*, second ed. CRC Press, Boca Raton, FL, pp. 135–191.

Sparks, D.L., 2003. *Environmental Soil Chemistry*, second ed. Academic Press, New York.

Sparks, D.L., Jardine, P.M., 1984. Comparison of kinetic equations to describe K–Ca in pure and mixed systems. *Soil Sci.* **138**, 115–122.

Sposito, G., 1996. *The Environmental Chemistry of Aluminum*, second ed. CRC press, London.

Stevenson, F.J., 1994. *Humus Chemistry*, second ed. John Wiley and Sons, New York.

Strawn, D.G., Scheidegger, A.M., Sparks, D.L., 1998. Kinetics and mechanisms of Pb(II) sorption and desorption at aluminum oxide–water interface. *Environ. Sci. Technol.* **32**, 2596–2601.

Stumm, W., Morgan, J.J., 1996. *Aquatic Chemistry. Chemical Equilibria and Rates in Natural Waters*. John Wiley and Sons, New York.

Taniguchi, S., Yamagata, N., Sakurai, K., 2000. Cadmium adsorption on hydroxyaluminosilicate–montmorillonite complex as influenced by oxalate and citrate. *Soil Sci. Plant. Nutr.* **46**, 315–324.

Violante, A., Pigna, M., 2002. Factors affecting the competitive sorption of phosphate and arsenate on different clay minerals and soils. *Soil Sci. Soc. Am. J.* **66**, 1788–1796.

Violante, A., Ricciardella, M., Pigna, M., 2003. Adsorption of heavy metals on mixed Fe–Al oxides in the absence or presence of organic ligands. *Water, Air Soil Pollut.* **145**, 289–306.

Violante, A., Huang, P.M., 1984. Characteristics and surface properties of pseudoboehmites formed in the presence of selected organic and inorganic ligands. *Soil Sci. Soc. Amer. J.* **48**, 1193–1201.

Violante, A., Huang, P.M., 1985. Influence of inorganic and organic ligands on the formation of aluminum hydroxides and oxyhydroxides. *Clays Clay Miner.* **33**, 181–192.

Violante, A., Huang, P.M., 1989. Influence of oxidation treatments on surface properties and reactivities of short range ordered products of aluminum. *Soil Sci. Soc. Am. J.* **53**, 1402–1407.

Violante, A., Huang, P.M., 1993. Formation mechanism of aluminum hydroxide polymorphs. *Clays Clay Miner.* **41**, 590–597.

Violante, A., Krishnamurti, G.S.R., Huang, P.M., 2002. Impact of organic substances on the formation and transformation of metal oxides in soil environments. In: Huang, P.M., Bollag, J.-M., Senesi, N. (Eds.), *Interactions between Soil Particles and Microorganisms*. John Wiley and Sons, Chichester, UK, pp. 133–171.

Violante, A., Violante, P., 1980. Influence of pH, concentration and chelating power of organic anions on the synthesis of aluminum hydroxides and oxyhydroxides. *Clays Clay Miner.* **28**, 425–434.

Wang, D., Anderson, D.W., 1998. Direct measurement of organic carbon content in soils by the Leco 12 Carbon Analyzer. *Soil Soc. Plant Anal.* **28**, 26–31.

Zou, W., Han, R., Chen, Z., Zhang, J., Shi, J., 2006. Kinetic study of adsorption of Cu(II) and Pb(II) from aqueous solutions using manganese oxide coated zeolite in batch mode. *Colloids and Surfaces A: Physicochem. Eng. Aspects* **279**, 238–246.